The Cryosphere, 10, 1433–1448, 2016
www.the-cryosphere.net/10/1433/2016/
doi:10.5194/tc-10-1433-2016

The Cryosphere Open Access EGU

Glacier melting and precipitation trends detected by surface area changes in Himalayan ponds

Franco Salerno[1,3], Sudeep Thakuri[1,3], Nicolas Guyennon[2], Gaetano Viviano[1], and Gianni Tartari[1,3]

[1]National Research Council, Water Research Institute (IRSA-CNR), Brugherio, Italy
[2]National Research Council, Water Research Institute (IRSA-CNR), Rome, Italy
[3]Ev-K2-CNR Committee, Via San Bernardino, 145, Bergamo 24126, Italy

Correspondence to: Franco Salerno (salerno@irsa.cnr.it)

Received: 8 February 2016 – Published in The Cryosphere Discuss.: 22 March 2016
Revised: 14 June 2016 – Accepted: 15 June 2016 – Published: 11 July 2016

Abstract. Climatic time series for high-elevation Himalayan regions are decidedly scarce. Although glacier shrinkage is now sufficiently well described, the changes in precipitation and temperature at these elevations are less clear. This contribution shows that the surface area variations of unconnected glacial ponds, i.e. ponds not directly connected to glacier ice, but that may have a glacier located in their hydrological basin, can be considered as suitable proxies for detecting past changes in the main hydrological components of the water balance. On the south side of Mt Everest, glacier melt and precipitation have been found to be the main drivers of unconnected pond surface area changes (detected mainly with Landsat imagery). In general, unconnected ponds have decreased significantly by approximately 10 ± 5 % in terms of surface area over the last 50 years (1963–2013 period) in the study region. Here, an increase in precipitation occurred until the mid-1990s followed by a decrease until recent years. Until the 1990s, glacier melt was constant. An increase occurred in the early 2000s, while a declining trend in maximum temperature has caused a reduction in the glacier melt during recent years.

1 Introduction

Meteorological measurements in high-elevation Himalayan regions are scarce due to the harsh conditions of these environments and their remoteness, which limit the suitable maintenance of weather stations (e.g. Vuille, 2011; Salerno et al., 2015). Consequently, the availability of long series is even more rare (Barry, 2012; Rangwala and Miller, 2012; Pepin et al., 2015). Generally, gridded and reanalysis meteorological data are used to overcome this lack of data and can be considered as an alternative (e.g. Yao et al., 2012). However, in these remote environments, their use in climate change impact studies at the synoptic scale must be done with caution due to the absence of weather stations across the overall region, which limits the ability to perform land-based evaluations of these products (e.g. Xie et al., 2007). Consequently, the meager knowledge on how the climate has changed in recent decades in high-elevation Himalayan regions presents a serious challenge to the interpretation of the relationships between causes and recently observed effects on the cryosphere. Although glacier reduction in the Himalayas is now sufficiently well described (Bolch et al., 2012; Yao et al., 2012; Kääb et al., 2012), the manner in which changes in climate drivers (precipitation and temperature) have influenced the shrinkage and melting processes is less clear (e.g. Bolch et al., 2012; Salerno et al., 2015), and this lack of understanding is amplified when forecasts are conducted.

In this context, the recent literature has already demonstrated the high sensitivity of lakes and ponds to climate (e.g. Pham et al., 2008; Williamson et al., 2008; Adrian et al., 2009; Lami et al., 2010). Some climate-related signals are highly visible and easily measurable in lakes. For example, climate-driven fluctuations in lake surface areas have been observed in many remote sites. Smol and Douglas (2007a) reported decadal-scale drying of high Arctic ponds due to changes in the evaporation/precipitation ratio. Smith et al. (2005), among other authors, found that lakes in areas of discontinuous permafrost in Alaska and Siberia have dis-

appeared in recent decades. In the Italian Alps, Salerno et al. (2014a) found that since the 1980s, lower elevation ponds have experienced surface area reductions due to increased evaporation / precipitation ratio for the effect of higher temperature, while higher elevation ponds have increased in size and new ponds have appeared as a consequence of glacial retreat.

In high mountain Asia and in particular in the interior of the Tibetan Plateau, the observed lake growth since the late 1990s is mainly attributed to increased precipitation and decreased evaporation (Lei et al., 2014; Song et al., 2015). In contrast, Zhang et al. (2015) attribute the observed increases in lake surface areas since the 1990s across the entire Pamir–Hindu Kush–Karakoram–Himalayas region and the Tibetan Plateau region to enhanced glacier melting. Wang et al. (2015) reached similar conclusions in a basin located in the south-central Himalaya. In our opinion, the divergences in the causes leading to the lake surface area variations in central Asia are due to the fact that different types of glacial lakes (described below) have been considered in these studies.

In general, in high mountain Asia, three types of glacial lakes can be distinguished according to Ageta et al. (2000) and Salerno et al. (2012): (i) lakes that are not directly connected with glacier ice but that may have a glacier located in their hydrological basin (unconnected glacial lakes); (ii) supraglacial lakes, which develop on the surface of a downstream portion of a glacier; and (iii) proglacial lakes, which are moraine-dammed lakes that are in contact with the glacier front. Some of these lakes store large quantities of water and are susceptible to glacial lake outburst floods (GLOFs). Factors controlling the growth of supraglacial lakes depend on the glacier features from which they develop (surface gradient, mass balance, cumulative surface lowering, and surface velocity) (Reynolds, 2000; Quincey et al., 2007; Sakai and Fujita, 2010; Salerno et al., 2012; Sakai, 2012; Thakuri et al., 2016). The causes of proglacial lake development are decidedly similar to those described for supraglacial lakes (e.g. Bolch et al., 2008; Salerno et al., 2012; Thakuri et al., 2016). Their filling and drainage are linked to the supply of meltwater from snow or glacial sources (Benn et al., 2001; Liu et al., 2015). In contrast, unconnected glacial lakes do not have a close dependence on glacier dynamics, and this aspect makes them potential indicators of the water balance components in high-elevation lake basins i.e. precipitation, glacier melting, and evaporation. These main contributions would best explain the causes of lake changes (e.g. Song et al., 2014; Wang et al., 2015; Salerno et al., 2015). A valuable opportunity for a fine-scale investigation on climate-driven fluctuations in lake surface area is particularly evident on the south slopes of Mt Everest (Nepal), which is one of the most heavily glacierized parts of the Himalayas (Scherler et al., 2011). Additionally, this region has the largest number of lakes in the overall Hindu-Kush-Himalayas range (Gardelle et al., 2011), and a 20-year series of temperature and precipitation data has recently been reconstructed for these high elevations (5000 m a.s.l.) (Salerno et al., 2015). Moreover, the relative small size of the water bodies in this region, which we can be defined as ponds according to Hamerlík et al. (2013) (a threshold of 2×10^4 m^2 exists between ponds and lakes), make them especially susceptible to the effects of climatic changes because of their relatively high surface area to depth ratios (Smol and Douglas, 2007b). This contribution examines the surface area changes of unconnected glacial ponds on the south side of Mt Everest (an example is shown in Fig. 1) during the last 50 years (1963–2013). This study aims to evaluate whether they might be used as a proxy to infer past spatial and temporal trends of the main components of the hydrological cycle (precipitation, glacier melting, and evaporation) at high elevations. Possible drivers of change are investigated through land climatic data, available in the area, and correlation analysis. Furthermore, morphological boundary conditions (glacier cover, pond size, pond location, basin aspect, basin elevation) are analysed as possible factors controlling the pond surface area changes. The study is concluded comparing gridded and reanalysis time series (evaluated vs. land climatic data) with observed pond surface area changes in the last 50 years.

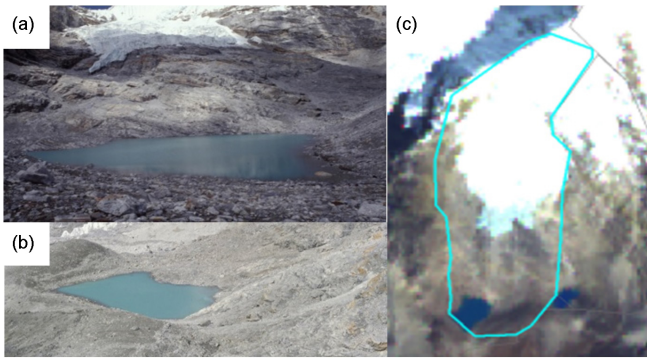

Figure 1. Example of an unconnected glacial pond (LCN5) with a glacier within the basin. Pictures were taken in September 1992 (Gabriele Tartari): **(a)** view looking north showing the distance between the glacier and the pond surface; **(b)** from east showing the frontal moraine. **(c)** LCN5 basin tracked on ALOS 2008 imagery.

2 Region of investigation

The current study is focused on the southern Koshi (KO) Basin, which is located in the eastern part of central Himalayas (Guzzella et al., 2016), (Fig. 2). In particular, the region of investigation is the southern slopes of Mt Everest in Sagarmatha (Mt Everest) National Park (SNP) (27°45′ to 28°7′ N; 85°59′ to 86°31′ E) (Fig. 2a) (Amatya et al., 2010; Salerno et al., 2010). The SNP (1148 km^2) is the highest protected area in the world, extending from an elevation of 2845 to 8848 m a.s.l. (Salerno et al., 2013). Land cover classifica-

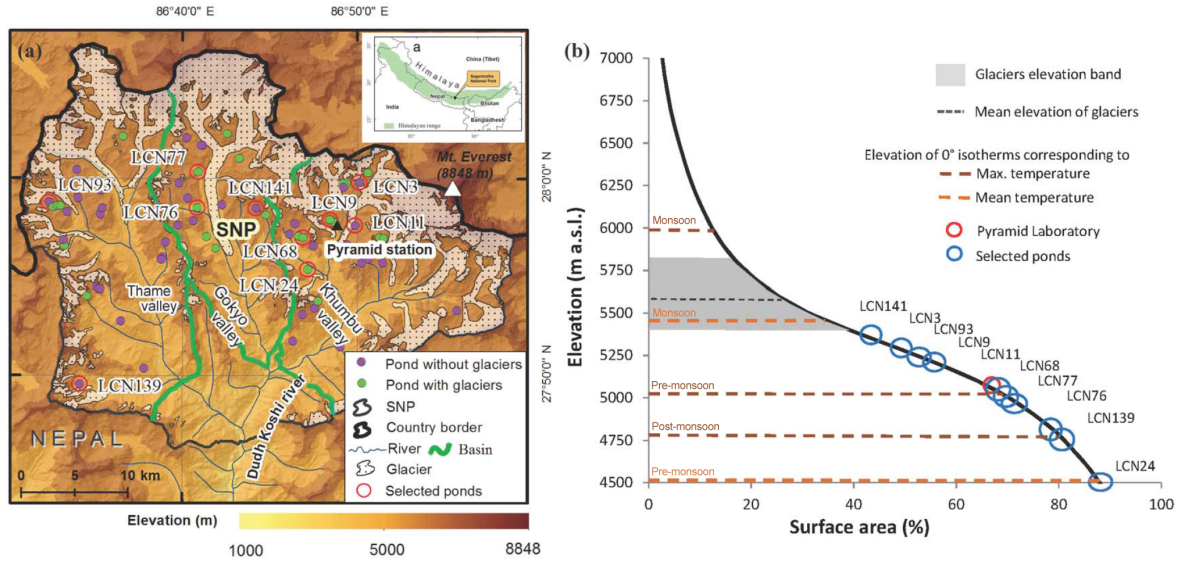

Figure 2. (a) Location of the study area in the Himalayas and a detailed map of the spatial distribution of all 64 unconnected ponds considered in this study. **(b)** Hypsometric curve of SNP. Along this curve, the locations of 10 selected ponds are shown. The 0 °C isotherms corresponding to the mean and maximum temperature in 2013 are plotted for the pre-, post-, and monsoon period according to the lapse rates reported in Salerno et al. (2015). The mean glacier elevation distribution (mean ± 1 standard deviation) of 10 selected ponds and the location of the Pyramid meteorological station are also reported.

tion shows that almost one-third of the territory contains temperate glaciers and less than 10 % is forested (Bajracharya et al., 2010), mainly with *Abies spectabilis* and *Betula utilis* (Bhuju et al., 2010).

The climate is characterized by monsoons, with a prevailing S–N direction (Ichiyanagi et al., 2007). For the 1994–2013 period at the Pyramid meteorological station (5050 m a.s.l.) (Fig. 2a), the total annual accumulated precipitation is 446 mm, with a mean annual temperature of −2.45 °C. In total, 90 % of the precipitation falls between June and September. The probability of snowfall during these months is very low (4 %) but reaches 20 % at the annual level. Precipitation linearly increases to an elevation of 2500 m and exponentially decreases at higher elevations (Salerno et al., 2015; Derin et al., 2016).

Most of the large glaciers in the SNP are debris-covered; i.e. the ablation zone is partially covered with supraglacial debris (e.g. Scherler et al., 2011; Bolch et al., 2011; Thakuri et al., 2014). However, the glaciers located within the considered pond basins are very small, steep, and cling to the mountain peaks; and thus they did not develop a debris-covered ablation area. The glacier surfaces are distributed from approximately 4300 to above 8000 m a.s.l., with more than 75 % of the glacier surfaces lying between 5000 and 6500 m a.s.l. The area-weighted mean elevation of the glaciers is 5720 m a.s.l. in 2011 (Thakuri et al., 2014). Glaciers in this region are identified as summer-accumulation glaciers that are fed mainly by summer precipitation from the South Asian monsoon system (Ageta and Fujita, 1996; Soncini et al., 2016).

Salerno et al. (2012) performed the complete inventory of lakes and ponds in the SNP by digitizing ALOS-08 imagery and assigning each body of water a numerical code (LCN, lake cadaster number) according to Tartari et al. (1998). They reported a total of 624 water bodies in the park, including 17 proglacial ponds, 437 supraglacial ponds, and 170 unconnected ponds. Previous studies revealed that the areas of proglacial ponds increased on the south slopes of Mt Everest after the early 1960s (Bolch et al., 2008; Tartari et al., 2008; Gardelle et al., 2011; Thakuri et al., 2016). Many studies have indicated that the current moraine-dammed or ice-dammed ponds are the result of coalescence and growth of supraglacial ponds (e.g. Fujita et al., 2009; Salerno et al., 2012). Such ponds pose a potential threat due to GLOFs. Imja Tsho (lake) is one of the proglacial lakes in the Everest region that developed in the early 1960s as a small pond and subsequently expanded continuously (Bolch et al., 2008; Somos-Valenzuela et al., 2014; Fujita et al., 2009; Thakuri et al., 2016).

3 Data and methods

3.1 Overall methodological approach

This section provides a brief description of the overall methodological approach applied in this study, whereas in the following sections, data and methods are described in detail.

An intra-annual analysis was carried out for throughout the year 2001 on a limited set of unconnected ponds for detecting the months characterized by the lowest surface area intra-annual variability and consequently the best period of the year to select the satellite images necessary for the inter-annual analysis.

An inter-annual analysis was carried out for the 2000–2013 period (hereafter we refer to this analysis as *short-term inter-annual analysis*), considering the wide availability of satellite imagery in this period, on some selected unconnected ponds (hereafter we refer to these ponds as *selected ponds*) to continuously track the inter-annual variations in surface area. This analysis aims to investigate the possible drivers of change (precipitation, evaporation, and glacier melt) considering the availability of continuous series of annual pond surface areas and climatic data from a land station located in the area. The study has been carried out through correlation analysis and principal component analysis (PCA).

An inter-annual analysis was carried out for the 1963–2013 period (hereafter we refer to this analysis as *long-term inter-annual analysis*) on a wider unconnected pond population (hereafter we refer to this population as *all considered ponds*) and on glaciers located within their hydrological basin. Two kinds of analyses have been carried out on this set of data: (1) pond surface area changes have been related to certain morphological boundary conditions. This analysis allows the factors controlling the pond surface area changes to be investigated. The significance of the observed differences has been evaluated with specific statistical tests. (2) Pond surface area changes have been related to climatic data. This analysis aims to point out the capability of unconnected ponds to infer information on the detected drivers of change also in the past when land climatic data did not exist. This study needed a preliminary analysis to reconstruct the climatic trends before the year 1994. Selected regional gridded and reanalysis datasets have been compared with land weather data available for the 1994–2013 period.

3.2 Climatic data

The monthly mean of daily maximum, minimum, and mean temperature and monthly cumulated precipitation time series used in this study have been reconstructed for the elevation of the Pyramid Laboratory (5050 m a.s.l.) (Fig. 2) for the 1994–2013 period (Salerno et al., 2015). The potential evaporation for the period (2003–2013) has been calculated by applying the Jensen–Haise model (Jensen and Haise, 1963) using the mean daily air temperature and daily solar radiation recorded continuously during the 2003–2013 period at Pyramid Laboratory. The Jensen–Haise model is considered to be one of the most suitable evaporation estimation methods for high elevations (e.g. Gardelle et al., 2011; Salerno et al., 2012).

To obtain information on climatic trends in the antecedent period (before 1994), we used some regional gridded and reanalysis datasets. We selected the closest grid point to the location of the Pyramid Laboratory, and all data were aggregated monthly to allow for a comparison at the relevant timescale. With respect to precipitation, we test the monthly correlation between the Pyramid data and the GPCC (Global Precipitation Climatology Centre), APHRODITE (Asian Precipitation-Highly Resolved Observational Data Integration Towards Evaluation of Water Resources), ERA-Interim reanalysis of the European Centre for Medium-Range Weather Forecasts (ECMWF), and CRU (Climate Research Unit Time Series) datasets. For mean air temperature, we considered the ERA-Interim, CRU, GHCN (Global Historical Climatology Centre), and NCEP-CFS (National Centers for Environmental Prediction Climate Forecast System) datasets, whereas for maximum and minimum temperatures, we used the ERA-Interim and NCEP-CFS datasets (details on the gridded and reanalysis products are reported in Table S1 in the Supplement).

3.3 Pond digitization

3.3.1 Long-term inter-annual analysis

Pond surface areas were manually identified and digitized using a topographic map from 1963 and more recent satellite imagery from 1992 to 2013. The topographic map of the Indian survey of the year 1963 (hereafter TISmap-63, scale 1 : 50 000) was used to complement the results obtained from the declassified Corona KH-4 (15 December 1962, spatial resolution 8 m). Thakuri et al. (2014) described the co-registration and rectification procedures applied to the Corona KH-4 imagery. Unfortunately, on these satellite images many ponds are snow-covered. Therefore here we considered the ponds' surface area digitalized on TISmap-63. The accuracy of this map has been tested comparing the surface areas of 13 ponds digitalized on both data sources (favouring the cloud- and shadow-free ponds). Figure S1 in the Supplement shows the proper correspondence of these comparisons. Furthermore, in order to estimate the mean bias associated with TISmap-63, we calculated the mean absolute error (MAE) (Willmott and Matsuura, 2005) between data, of which the result was sufficiently low (3.6 %), in this way assuring the accuracy of ponds surface area digitalized on TISmap-63.

In total, five scenes were considered according to the availability of satellite imagery. Landsat images have been mainly used, except in 2008, when in the region the ALOS image, presenting a better resolution, was available (details on data sources are provided in Table S2).

We only tracked those ponds present continuously in all these five periods to exclude possible ephemeral water bodies. As described below, 64 ponds have been tracked from 1963 to 2013 (Fig. 2a).

3.3.2 Short-term inter-annual analysis

From the 2000 to 2013 period, due to a wider availability of satellite imagery (and in particular the Landsat imagery), 10 ponds were selected among the pond population (64 ponds) considered in the long-term analysis (1963–2013) to continuously track the inter-annual variations in surface area in the recent years. The largest ponds, free from cloud cover, and with diverse glacier coverages (from 1 to 32 %) within their hydrological basin, were favoured in the selection (details on data sources used for these ponds are provided in Table S3).

3.3.3 Intra-annual analysis

The intra-annual variability in pond surface area was investigated for throughout the year 2001 through the availability of five cloud-free satellite images from June to December (details on data sources used for these ponds are provided in Table S4). The first months of the year were excluded from the analysis because many ponds were frozen until April/May. Even in this case, the main criterion driving the ponds selection was the absence of cloud cover from the satellite images over the pixels representing the pond surface area. Only ponds for which a continuous series of data was retrieved from June to December were selected. Moreover the largest ponds were favoured in order to reduce the uncertainty in the shoreline delineation. Thus, four ponds were selected, and their intra-annual variability is tracked in Fig. 3. We observe a common significant increase in pond surface area during the summer months, likely due to monsoon precipitation and high glacier melting rates. This increase in surface area disappears on average during the fall. Some single ponds present a dispersion of around 5 % between October and December (LCN4 and LCN77). However, the same figure points out that just by averaging this information on a population only slightly larger, the dispersion between October and December becomes almost zero (1 %). Therefore these months are the best period to select the satellite images necessary for the inter-annual analysis of pond surface area. In fact, during these months, the ponds are not yet frozen, the sky is almost free from cloud cover, and, as observed in Fig. 3, the inter-annual analysis on average is not affected by intra-annual seasonality. Consequently all images for the inter-annual analysis have been selected from these months (Tables S1, S2). Generally, climatic inferences coming from the analysis of surface area of ponds surely need to consider a wider number of ponds in order to reduce the intra-annual variability due to the local conditions of each lake.

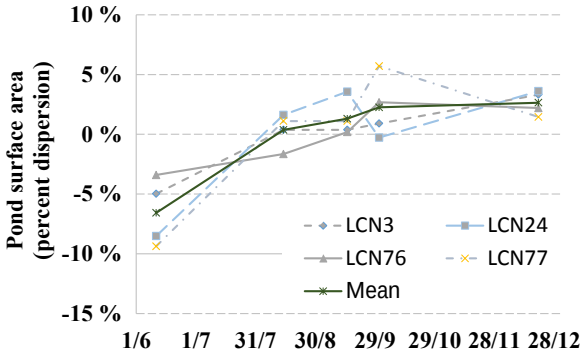

Figure 3. Intra-annual analysis (June–December) of selected pond surface areas. Percent dispersions are computed dividing the anomalies by the mean.

3.4 Glacier surface areas and melt

Glacier surface areas within the basins containing the ponds were derived from the Landsat 8 remote imagery (10 October 2013) taken by the Operational Land Imager (OLI) with a resolution of 15 m. The satellite imagery used to track the inter-annual variations in glaciers since the early 1960s is reported in Table S2. Detailed information on digitization methods are described in Thakuri et al. (2014).

To simulate the daily melting of the glaciers associated with the 10 selected ponds, we used a simple T-index model (Hock, 2003). This model is able to generate daily melting discharges as a function of daily air temperature above zero, the glacier elevation bands (using the digital elevation model – DEM – described below), and a melt factor ($0.0087\,\mathrm{m\,d^{-1}\,^{\circ}C^{-1}}$) provided by Kayastha et al. (2000) from a field study (Glacier AX010) located close to the SNP (southwest). The Glacier AX010 glacier is a small debris-free glacier, located in the Dudh Koshi valley in the same climatic and geographic setting of glaciers considered here. The choice of using a simple model of melting is due to the fact that this paper does not have the specific objective to provide an accurate evaluation of the magnitude of the meltwater released from glaciers located in the pond basins, but rather to estimate its trend, as a function of the temperature, in order to evaluate whether the glacier melt is a possible driver of changes of the pond surface areas. Being interested in the melt trend and not in its absolute magnitude and considering that these small glaciers are ungauged, we do not need more sophisticated melt models, which consider specific geometries and differentiated melt factors.

The T-index model has been applied here considering the daily temperature of the Pyramid Laboratory corrected using the monthly lapse rates reported in Salerno et al. (2015) for each 50 m glacier elevation band. The melt estimated for each band has been then summed to calculate the total melt for each glacier.

3.5 Morphometric parameters

The parameters related to the ponds' basin as the area, slope, aspect, and elevation were calculated through the DEM derived from the ASTER GDEM (Tachikawa et al., 2011). The vertical and horizontal accuracy of the GDEM are ∼ 20

and ∼ 30 m, respectively (Tachikawa et al., 2011; Hengl and Reuter, 2011). We decided to use the ASTER GDEM instead of the Shuttle Radar Topography Mission (SRTM) DEM considering the higher resolution (30 and 90 m, respectively) and the large data gaps of the SRTM DEM in this study area (Bolch et al., 2011). Furthermore, the ASTER GDEM shows better performance in mountainous terrains (Frey et al., 2012). Hydrological basins have been digitalized using ArcGIS® hydrology tools as carried out by other authors (e.g. Pathak and Whalen, 2013). The circular statistic has been used for computing the (vector) mean and median values of glaciers and basins aspect (Fisher, 1993).

3.6 Uncertainty of measurements

All of the imagery and map were co-registered in the same coordinate system of WGS 1984 UTM Zone 45N. The Landsat scenes were provided in standard terrain-corrected level (Level 1T) with the use of ground control points (GCPs) and necessary elevation data (LANDSAT SPPA Team, 2015). The ALOS-08 image used here was orthorectified and corrected for atmospheric effects as described in Salerno et al. (2012).

Concerning the accuracy of the measurements, we refer mainly to the work of Tartari et al. (2008) and Salerno et al. (2012, 2014a) which address the problem of uncertainty in the morphometric measurements related to ponds and glaciers obtained from remote sensing imagery, maps, and photos in detail. The uncertainty in the measurement of a shape's dimension is dependent both upon the linear error (LE) and its perimeter. In particular for ponds, as discussed by many authors, only the linear resolution error (LRE) needs to be considered (e.g. Fujita et al., 2009; Gardelle et al., 2011). Therefore we did not consider the co-registration error because the comparison was not performed pixel by pixel, at the entity level (pond) (Salerno et al., 2012, 2015; Thakuri et al., 2016; Wang et al., 2015). The LRE is limited by the resolution of the source data. In the specific study of temporal variations of ponds, Fujita et al. (2009) and Salerno et al. (2012) assumed an error of ±0.5 pixels, assuming that on average the lake margin passes through the centres of pixels along its perimeter. The uncertainties in the changes in pond surface area were derived using a standard error propagation rule, i.e. the root sum of the squares (uncertainty $= \sqrt{e_1^2 + e_2^2}$), where e_1 and e_2 are uncertainties from the first and second scene of the mapping uncertainty in two scenes (Salerno et al., 2012; Thakuri et al., 2016).

3.7 Statistical analysis

In the short-term inter-annual analysis, the degree of correlation among the data was verified through the Pearson correlation coefficient (r) after testing that the quantile–quantile plot of model residuals follows a normal distribution (not shown here) (e.g. Venables and Ripley, 2002). All tests are implemented in the R software (R Development Core Team, 2008) with the significance level at $p < 0.05$. The normality of the data is tested using the Shapiro–Wilk test (Shapiro and Wilk, 1965; Hervé, 2015). Razali and Waph (2011) demonstrate that the Shapiro–Wilk test presents the highest power for small sample size. The data were also tested for homogeneity of variance with the Levene's test (Fox and Weisberg, 2011). All comparisons conducted in this study are homoscedastic.

To evaluate the significance of differences in surface area changes of ponds' population, both in time and in respect to certain morphological boundary conditions, some parametric and non-parametric tests have been used. We applied the paired t-test to compare the means of two normally distributed series. If the series were not normal, as a non-parametric analysis of variance (ANOVA), we used the Friedman test for paired comparisons and the post-hoc test according to Nemenyi (Pohlert, 2014), while for non-paired comparisons we applied the Kruskal–Wallis test and the post-hoc test according to Nemenyi–Damico–Wolfe–Dunn (Hothorn et al., 2015). The significance of the temporal trends has been tested using the Mann–Kendall test ($p < 0.10$) (Mann, 1945; Kendall, 1975; Guyennon et al., 2013). When a time series is not very long, the associated significance level should be considered with caution.

We conducted principal component analysis (PCA) as described in Wold et al. (1987) between pond surface area variations and climatic variables to obtain information on relationships among the data and to look for reasons that could justify the observed changes in the pond size (e.g. Settle et al., 2007; Salerno et al., 2014a, b; Viviano et al., 2014).

4 Results

4.1 Pond and glacier surface area variations

Among the 170 unconnected ponds inventoried in the 2008 satellite imagery (Salerno et al., 2012) in the SNP, we tracked, according to the criteria described above, a total of 64 ponds (approximately 1/3) (Fig. 2a). Table 2 provides a general summary of their morphological features. We use the median values to describe these water bodies because, in general, we observed that these morphological data do not follow a normal distribution. The population consists of ponds larger than approximately 1 ha (1.1×10^4 m^2), located on relatively steep slopes (27°), and mainly oriented towards south–southeast (159°). These ponds are located at a median elevation of 5181 m a.s.l. and within an elevation zone ranging from 4460 to 5484 m a.s.l. The observed changes in the surface area of all the considered ponds are listed in Table 3. In general, all unconnected ponds decreased by approximately 10 ± 5 % in surface area in the last 50 years (1963–2013), with a significant difference based on the Friedman test ($p < 0.01$). Figure 4d and Table 3 show that, until the

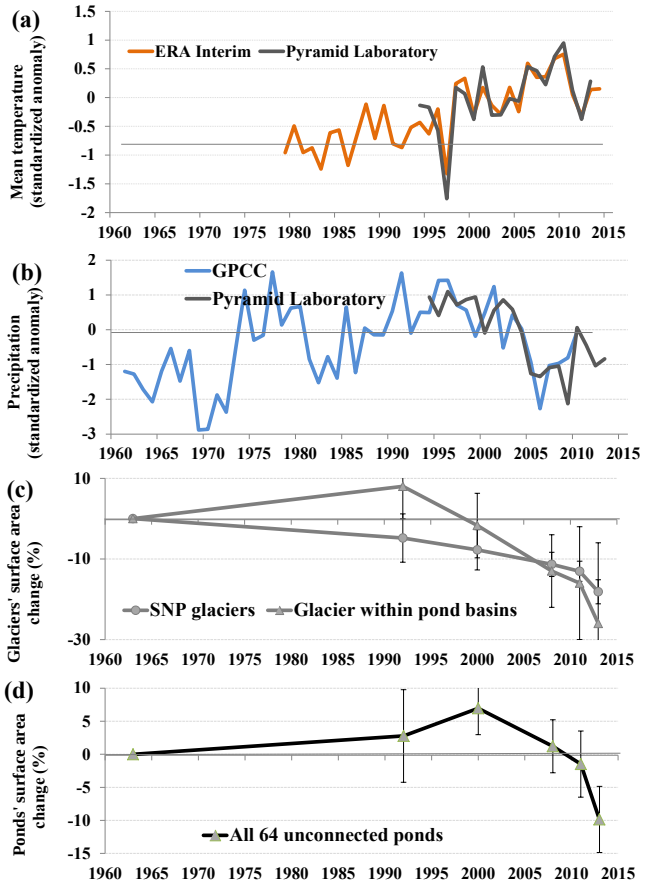

Figure 4. Trend analysis of climate and glaciers' and ponds' surface area for the last 50 years in the SNP: **(a)** ERA-Interim mean annual temperature compared with Pyramid's land-based data; **(b)** GPCC annual precipitation and Pyramid's land-based data; **(c)** glacier surface area variations for the overall SNP (Thakuri et al., 2014) and for glaciers located in basins of 64 considered ponds. **(d)** Surface area variations of all 64 considered ponds. *Y* axis units: **(a)** and **(b)** trends are expressed in terms of standardized anomalies divided by the standard deviation (dimensionless); **(c)** and **(d)** relative variations with respect to 1963. Errors bars represent the uncertainty of measurements.

2000s, the ponds had a slight but not significant increasing trend ($+7 \pm 4\,\%$, $p > 0.05$). Since 2000, they have decreased significantly ($-1.7 \pm 0.6\,\%\,\mathrm{yr}^{-1}$, $p < 0.001$ corresponding to $-22 \pm 18\,\%$).

As for glaciers, Fig. 4c reports the glacier surface area changes observed across the SNP (approximately $400\,\mathrm{km}^2$) observed by Thakuri et al. (2014). They reported a decrease of $-13 \pm 3\,\%$ from 1963 to 2011. We updated this series to 2013 and found loss of surface area of $-18 \pm 3\,\%$. For the glaciers located in the basins containing the considered ponds, we tracked changes that were slightly larger. Their overall surface was $32.2\,\mathrm{km}^2$ in 1963 and $25.0\,\mathrm{km}^2$ in 2013, with a decrease of $-26 \pm 20\,\%$ (Fig. 4c; Table 3). According to many authors (e.g. Loibl et al., 2014), as we observe here, the main losses in area over the last decades in the Himalayas have been observed in smaller glaciers.

5 Discussion

5.1 Short-term inter-annual analysis: investigation on potential drivers of change

Considering the wide availability of satellite imagery during the 2000–2013 period, an inter-annual analysis has been carried out on 10 selected ponds in order to investigate the possible drivers of change. This was made possible exploiting the continuous series of annual pond surface areas on the one side, and climatic data from Pyramid station on the other.

5.1.1 Trends in pond surface areas

Table 4 provides the morphometric characteristics of 10 selected ponds. We observe that the median features of these ponds are comparable with the entire pond population (Table 2), highlighting the good representativeness of the selected case studies. Figure S2 shows, for each pond, the annual surface area variations that occurred during the 2000–2013 period. All the selected ponds show a significant ($p < 0.05$) decreasing trend according to what has been observed for the whole pond population during the same period.

5.1.2 Trends in possible drivers of change

The selected possible drivers of change are temperature (daily maximum, minimum and mean), precipitation, potential evaporation, and glacier melt of the pre-monsoon, monsoon (Fig. 5), and post-monsoon seasons. Pyramid data have been used for computing or aggregating these variables. The assumption behind this analysis is that these series can be considered representative both along the altitudinal gradient and in the different valleys of the SNP. The scarcity of land weather data at these elevations makes this assumption licit; although, at this regard, the detected drivers of change will be analysed in this respect in the last paragraph.

All these trends are noted in Fig. S3, and a correlation table comparing pond surface area variations and potential drivers of change is presented in Table S5. In general, we observe from this table that the highest correlations are found for the monsoon period. The reason is because 90 % of the precipitation and the highest temperatures are recorded during this period (Salerno et al., 2015). Consequently, the main hydrological processes in the Himalayas occur during the monsoon season. Focusing on this season, we first observe a large and significant precipitation decrease ($-11\,\mathrm{mm\,yr}^{-1}$; $p < 0.1$) from Fig. S3. Even the mean temperature decreases, but slightly and not significantly. This is a result of a significant decrease in maximum temperature ($-0.08\,^{\circ}\mathrm{C\,yr}^{-1}$; $p < 0.05$) balanced by an increase in minimum temperature. The potential evaporation, calculated on the basis of the mean

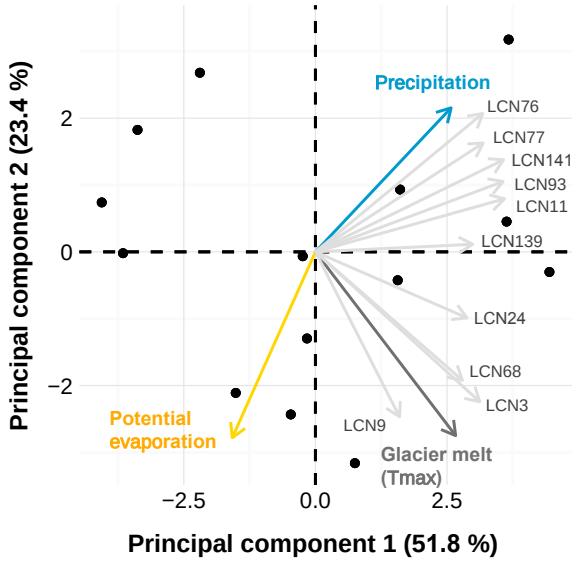

Figure 5. Principal component analyses (PCAs) between pond surface area from 2000 to 2013 and potential drivers of change (precipitation, glacier melt, and potential evaporation) related to the monsoon season. Coefficients of correlation are reported in Table S5. All trends related to ponds and variables are provided in Figs. S5 and S6.

temperature and global radiation, is constant during the summer period. These trends have been more broadly discussed in Salerno et al. (2015). They observed, for a longer period (since 1994), that the mean air temperature has increased by 0.9 °C ($p < 0.05$) at the annual level. However, the warming has occurred mainly outside the monsoon period and mainly in the minimum temperatures. Moreover, as we observed here for the 2000–2013 period, a decrease in maximum temperature from June to August ($-0.05\,°C\,yr^{-1}$, $p < 0.1$) has been observed. In terms of precipitation, a substantial reduction during the monsoon season (47 %, $p < 0.05$) has been observed.

The glacier melt related to each glacier within the pond basins has been calculated considering both maximum and mean daily temperature. The averages for all selected cases are analysed for each season in Fig. S3, which reveals that the only period producing a sensible contribution is the monsoon period if the maximum daily temperatures are considered the main driver of the process. The reason can be easily observed in Fig. 2b, which shows the 0 °C isotherms corresponding to the mean and maximum temperatures. Only the 0 °C isotherm related to the daily maximum temperature during the monsoon period is located higher than the mean elevation of the analysed glaciers. The T-index model only calculates the melting associated with temperatures above 0 °C, thereby explaining this pattern. In other words, the diurnal temperatures influence the melting processes much more than the nocturnal ones, which are considered in the mean daily temperature. Figure 6b shows that the trend is significantly decreasing ($3\,\%\,yr^{-1}$, $p < 0.05$), according to the decrease observed in maximum temperature.

5.1.3 Detection of drivers of change

As anticipated, the highest correlations pond surface areas are found for the monsoon period. Based on Table S5, we observe that precipitation, maximum temperature, and glacier melt (calculated from temperature) are the more correlated variables. The PCA shown in Fig. 5 attempts to provide an overall overview of the relationships, during the monsoon period, among the trends related to the potential drivers of change and the pond surface areas. This representation helps to further summarize the main components of the water balance system that influence the pond surface areas, i.e. glacier melt and precipitation. We observe that evaporation is not an important factor at these elevations, and that the evaporation / precipitation ratio is approximately 0.41. Therefore, a hypothetical variation in the precipitation regime affects the pond water balance 2.5 times more than the same variation in the evaporation rate. Moreover, from Fig. 5, we observe that there are some ponds that are more correlated with the monsoon precipitation (i.e. LCN76, LCN141, LCN77, LCN11, and LCN93) and others that are more correlated with the glacier melt (i.e. LCN68, LCN3, and LCN9). A few ponds seem influenced by both drivers (i.e. LCN24 and LCN139). The coefficients of correlation are reported in Table 4. According to the grouping observed with the PCA.

Figure 6 shows good fits between the pond surface area trends and the main drivers of change. Based on Table 4, ponds with higher glacier coverage within the basin show higher correlations with the glacier melt, and, in contrast, ponds with lower glacier coverage show higher correlations with precipitation; i.e. the glacier coverage is the discriminant variable. In our case study, the threshold between the two groups appears to be a glacier coverage of 10 %.

5.2 Long-term inter-annual analysis

An inter-annual analysis has been carried out from 1963 to 2013 for all 64 considered ponds in order to investigate (1) which morphological boundary conditions control the pond surface area changes and (2) the capability of unconnected ponds to infer information on the detected drivers of change also in the past when land climatic data did not exist.

5.2.1 Morphological boundary conditions controlling the pond surface area changes

We analysed whether all 64 considered ponds experienced changes in surface area in relation to certain morphological boundary conditions, such as the mean elevation of the basin, the pond surface area, the main three valleys of SNP (Fig. 2a), and the glacier cover. In this case, evaluating the normality of data, we apply the ANOVA test as well as the relevant post-hoc test described above. Figure S4 shows the

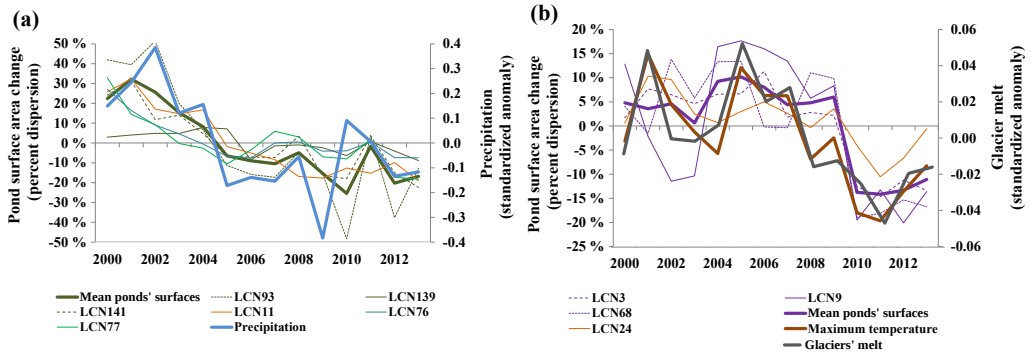

Figure 6. Annual trends from 2000 to 2013 related to pond surface area grouped according to the relevant main drivers of change (monsoon season): **(a)** precipitation, **(b)** glacier melt. Coefficients of correlation are reported in Table S5. All trends related to ponds and variables are provided in Figs. S5 and S6. Standardized anomalies (dimensionless) are computed dividing the anomalies by the standard deviation. Percent dispersions are computed dividing the anomalies by the mean.

surface area changes observed during the 1992–2013 period vs. morphological factors. The same analysis has also been carried out for the 1963–1992 period, reporting decidedly similar results (not shown here). We observe that the pond surface area changes are independent from elevation, valley, and pond size, whereas significant differences can be observed between ponds with and without glacier cover. In particular, ponds with glaciers experienced a lower surface area reduction. This analysis reconfirms that the glacier cover at these altitudes is the main discriminant parameter in the hydrological cycle of unconnected ponds.

We now analysed whether ponds with and without glacier cover within their hydrological basin experienced changes in surface area in relation to the aspect and the elevation of the basin. The two classes have been defined according to the observed threshold of 10 %. Hereafter, we define these ponds as ponds without glaciers in the basin, neglecting in this way relatively small glacier bodies, which could possibly be confused with snow fields. The opposite class is defined as ponds with glaciers in the basin. Among ponds with glaciers, Table 2 shows that they are characterized by a median glacier coverage of 19 %, oriented toward the east–southeast and relatively steep (31°). The observed changes according to this new classification are reported in Table 3.

In this analysis, we apply the Kruskal–Wallis test as the relevant post-hoc test described above. Figure 7 shows the surface area changes observed during the 1992–2013 period. The changes were independent of both elevation and aspect for ponds without glaciers (Fig. 7a, c), whereas significant differences can be observed for ponds with glaciers. Ponds located at higher elevations experienced greater decreases (Fig. 7b). In particular, ponds over 5400 m a.s.l. decreased significantly ($p < 0.01$) more than ponds located below 5100 m a.s.l. In terms of aspect, the south-oriented ponds (Fig. 7d) experienced greater decreases, which was significantly different from southeast ($p < 0.01$) and southwest ($p < 0.01$) orientations.

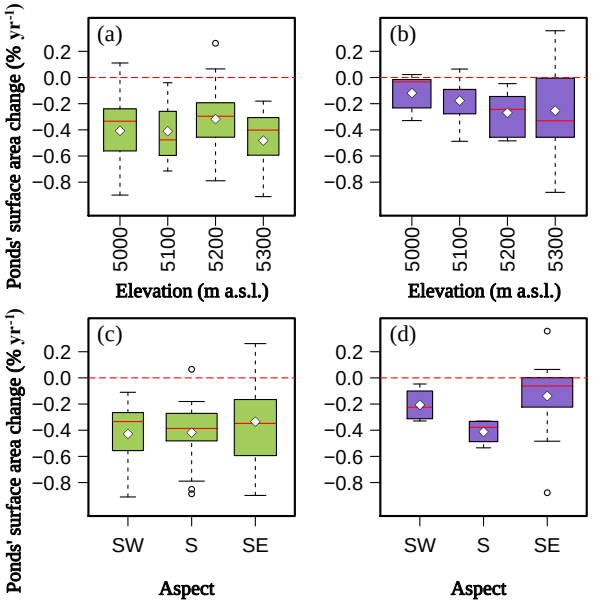

Figure 7. Pond surface area changes observed during the 1992–2013 period in relation to certain morphological boundary conditions in the basin: elevation (upper graphs) and aspect (lower graphs). On the left, ponds without glaciers are shown, and on the right, ponds with glaciers. The white points in the box plots indicate the mean, whereas the red lines indicate the median.

The tracking of pond surface area provides important information on precipitation and glacier melt trends in space. Ponds without glaciers allow us to understand that precipitation in the SNP generally occurs homogeneously at all elevations and in all valleys independent of the orientation (Fig. 7a, c). Based on the greater loss of surface area for ponds with glaciers at lower elevations, we can infer that glacier melt is actually higher at these elevations, surely due to the effect of higher temperatures (Fig. 7b). Even in valleys oriented in directions other than south, we observe greater

Table 1. Coefficients of correlation between precipitation and temperature time series recorded at Pyramid station for the 1994–2013 period and gridded and reanalysis datasets (pre-monsoon, monsoon, and post-monsoon seasons as the months of February–May, June–September, and October–January, respectively). Bold values are significant with $p < 0.01$.

		APHRODITE	GPCC	CRU	ERA-Interim
Precipitation	annual	0.43	**0.75**	0.34	0.33
		NCEP CFS	GHCN	CRU	ERA-Interim
Minimum temperature	pre-monsoon	**0.64**	–	–	**0.81**
	monsoon	0.47	–	–	**0.72**
	post-monsoon	**0.70**	–	–	**0.65**
	annual	**0.72**	–	–	**0.92**
Mean temperature	pre-monsoon	**0.79**	**0.83**	**0.8**	**0.87**
	monsoon	0.61	0.51	0.42	**0.67**
	post-monsoon	**0.79**	**0.77**	0.57	**0.82**
	annual	**0.81**	**0.85**	**0.89**	**0.92**
Maximum temperature	pre-monsoon	**0.83**	–	–	**0.88**
	monsoon	0.54	–	–	0.45
	post-monsoon	**0.82**	–	–	**0.86**
	annual	**0.70**	–	–	**0.80**

losses in surface area for ponds with glaciers (Fig. 7d). Small glaciers lying in perpendicular valleys, which are much steeper than the north–south-oriented valleys (following the monsoon direction), likely melt more due to their small size and higher gravitational stresses (e.g. Bolch et al., 2008; Quincey et al., 2009).

5.2.2 Pond surface areas as proxy of past changes of the hydrological cycle

Climate reconstruction

To reconstruct the climatic trends before 1994, we compared the annual and seasonal precipitation and temperature time series which have been recorded at Pyramid station since 1994 (Salerno et al., 2015) with selected regional gridded and reanalysis datasets (Table S1). Table 1 shows the coefficient of correlation found for these comparisons. ERA-Interim ($r = 0.92$, $p < 0.001$) for mean temperature (Fig. 4a) and GPCC ($r = 0.92$, $p < 0.001$) for precipitation (Fig. 4b) provide the best performance at the annual level. Figure S5 shows the location of ERA-Interim and GPCC nodes close to the region of investigation and in particular in relation to the Pyramid station. The comparisons between gridded/reanalysis and land data are visualized in Fig. S6. We observe that precipitation increased significantly until the middle 1990s (+25.6 %, $p < 0.05$, 1970–1995 period), then it started to decrease significantly (−23.9 %, $p < 0.01$, 1996–2010 period), as observed by the Pyramid station and described by Salerno et al. (2015). The mean temperature reveals a continuous increasing trend ($+0.039\,^{\circ}\mathrm{C\,yr^{-1}}$, $p < 0.001$, 1979–2013 period) that has accelerated since the early of 1990s.

Furthermore, Table 1 shows the low capability of all the products to correctly simulate monsoon temperatures and in particular the daily maximum ones. Figure S7a reports the correlations at monthly level for maximum temperature visually, while Fig. S7b highlights the misfit in the time between the maximum, mean, and minimum temperature trends during the monsoon period.

Analysis of ponds surface area in the last 50 years

The maps in Fig. 8 show the spatial differences between the two pond classes and compare the relative annual rate of change. Generally, no difference can be observed at valley level, as confirmed by the test applied above (Fig. S4). It is interesting to visually observe that most of the ponds without glaciers increased in the 1963–1992 period, while ponds with glaciers increased in the 1992–2000 period. Almost all the considered ponds decreased during the 2000–2013 period.

Figure 9 tracks their trends over time. We have already discussed (Fig. 4d) that, in general, all unconnected ponds over the last 50 years have decreased by approximately 10 %. Additionally, the presence of glaciers within the pond basins results in divergent trends. The surface area of ponds without glaciers strongly decreased (-25 ± 6 %, $p < 0.001$), from 1963 to 2013 (Fig. 9a). In contrast, the surface area of ponds with glaciers decreased much less (-6 ± 2 %, $p < 0.05$) for the same period (Fig. 9b). Differences in behaviour are also noticeable among the periods pointed out in Table 3. In this case, we compare the median values of the relative annual rates of change. From 1963 to 1992, ponds without glaciers increased slightly ($0.9 \pm 0.5\,\%\,\mathrm{yr^{-1}}$, $p < 0.1$), whereas the other ones remained constant ($0.0 \pm 0.1\,\%\,\mathrm{yr^{-1}}$). From 1992 to 2000, ponds with-

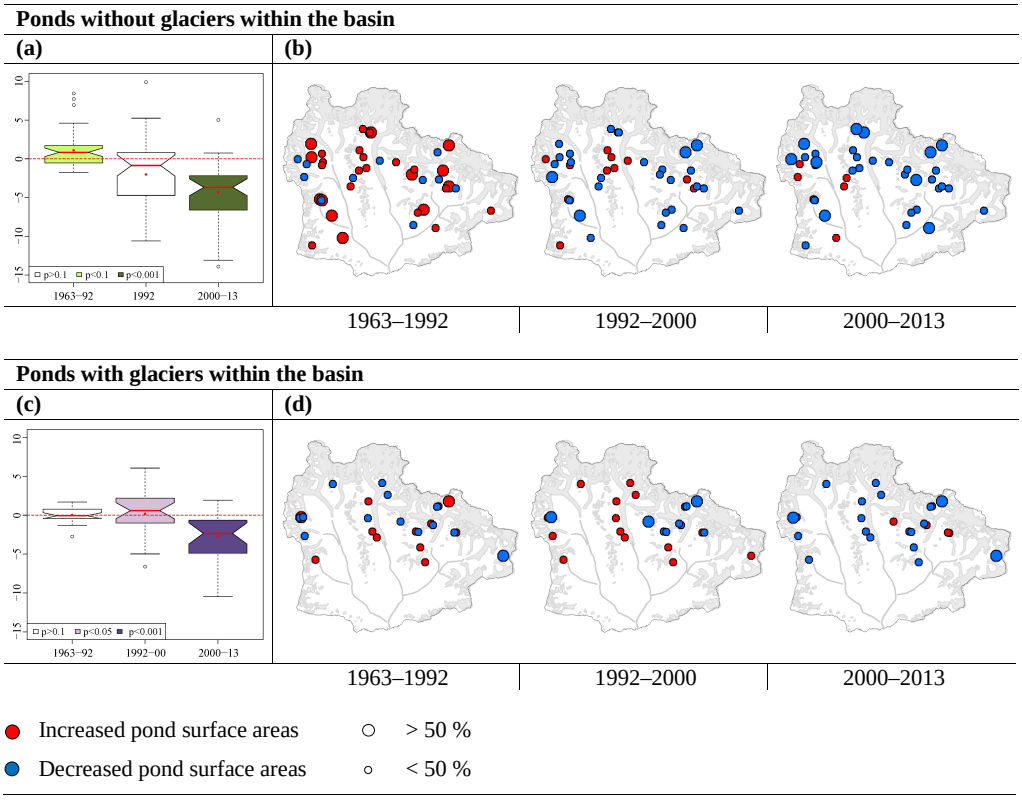

Figure 8. Changes in pond surface area in the Mt Everest region. The left box plots represent the annual rates of change of ponds in the analysed periods: **(a)** ponds without glaciers within the basin, **(c)** ponds with glaciers within the basin. The red points in the box plots indicate the mean, whereas the red lines indicate the median. Data are expressed in % yr^{-1}. On the right side, the maps **(b, d)** visualize the variations that occurred in the pond population during the same three periods considered in the relevant box plots on the left. Reference data are reported in Table 3. All percentages refer to the initial year of the analysis (1963).

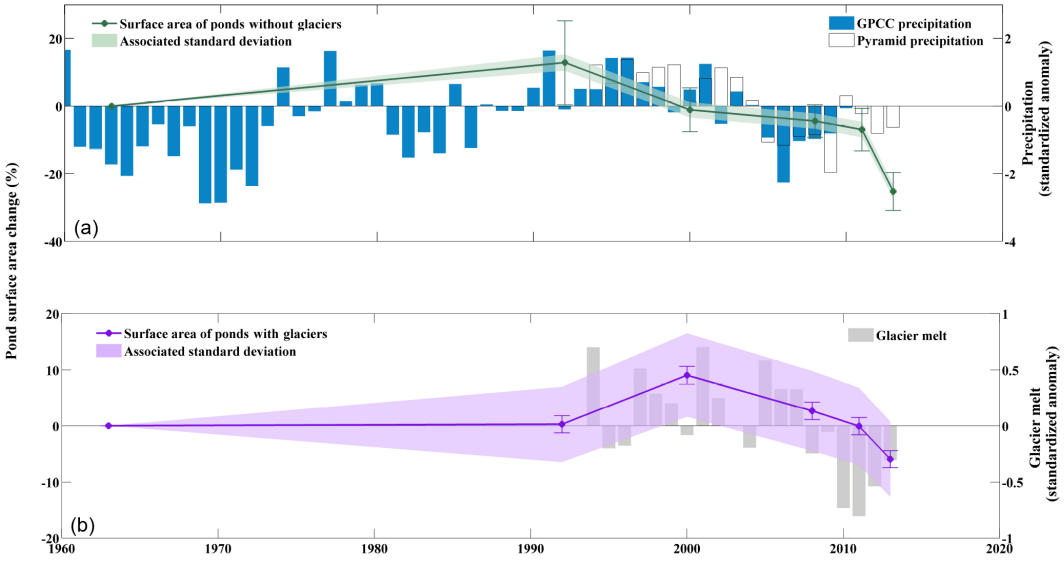

Figure 9. Comparison for the last 50 years between the annual precipitation and the glacier melt with the surface areas for **(a)** ponds without glaciers and **(b)** ponds with glaciers. Standardized anomalies (dimensionless) are computed by dividing the anomalies by the standard deviation. Error bars represent the uncertainty of measurements.

Table 2. General summary of the morphological features of all 64 considered ponds (data from 2013). Ponds are grouped according to the glacier cover present into each pond basin.

Topography	Glacier cover < 10 % median (range)	Glacier cover > 10 % median (range)	All lakes median (range)
Pond elevation (m a.s.l.)	5181 (4460–5484)	5159 (4505–5477)	5170 (4460–5484)
Pond area (10^4 m^2)	0.8 (0.1–6.2)	1.3 (0.3–56.3)	1.1 (0.1–56.3)
Basin area (10^4 m^2)	30 (2–430)	130 (30–2300)	70 (2–2300)
Basin slope (°)	25 (10–39)	29 (23–41)	27 (10–41)
Basin aspect (°)	163 (68–256)	141 (94–280)	159 (68–280)
Basin mean elevation (m a.s.l.)	5293 (4760–5531)	5400 (5119–5945)	5315 (4760–5945)
Basin / pond area ratio (m^2/m^2)	60 (3–485)	67 (10–523)	64 (3–523)
Glacier area (%)	0 (0–9)	19 (10–61)	0.5 (0–61)
Glacier slope (°)	–	31 (21–38)	–
Glacier aspect (°)	–	166 (150–250)	–
Glacier mean elevation (m a.s.l.)	–	5680 (5470–7500)	–

Table 3. General summary of surface area changes related to all 64 considered ponds from 1963 to 2013. The surface area changes of the glaciers located within the basins are also reported. For each comparison the uncertainty of measurement is also shown. On the right the cumulative loss in respect to 1963 is reported for each intermediate period (these data are used for Fig. 8). On the left the relative annual rates are calculated (these data are used for Fig. 7). Bold values represent the main periods of analysis.

Period	Pond surface area change				Period	Pond surface area change		
	Cumulative loss (%)					Relative annual rate (% yr^{-1})		
Glacier coverage	< 10%	> 10%	All ponds	All basins	Glacier coverage	< 10 %	> 10 %	All ponds
1963–1992	**+13±12**^{a}	**0±3**	**+3±7**	**8±8**	1963–1992	**0.9±0.5**^{a}	**0.0±0.1**	**+0.5±0.3**
1963–2000	−1± 6	+9 ± 2*	+7 ± 4	−2 ± 8	1992–2000	**−1.1±1.9**	**+0.7±0.5***	**−0.4±0.1**
1963–2008	−4± 5	+3 ± 2	+1 ± 4	−13 ± 9**	2000–2008	0.3 ± 1.0	−1.6 ± 0.6	−0.7 ± 0.7
1963–2011	−7± 6	0 ± 2	−2 ± 5	−14 ± 14**	2008–2011	0.0 ± 2.8	0.0 ± 1.6	0.0 ± 2.2
1963–2013	**−25±6*****	**−6±2***	**−10±5****	**−26±20****	2011–2013	12.9 ± 4.4***	−5.8 ± 2.5*	−11 ± 3.5**
1992–2013	**−38±6*****	**−6±2***	**−13±5****	**−34±15*****	2000–2013	**−2.3±0.7*****	**-1.5±0.4*****	**−1.7±0.6*****

Significance: *** $p < 0.001$, ** $p < 0.01$, * $p < 0.05$, ^{a} $p < 0.1$.

out glaciers decreased slightly (-1.1 ± 1.9 % yr^{-1}, $p > 0.1$), whereas the other ones increased slightly but significantly ($+0.7 \pm 0.5$ % yr^{-1}, $p < 0.05$). In the most recent period (2000–2013), both categories decreased, but ponds without glaciers decreased more (-2.3 ± 0.7 % yr^{-1}, $p < 0.001$; -1.5 ± 0.4 % yr^{-1}, $p < 0.001$).

The significance of the divergent trend observed between the two groups has been tested for two periods (1963–1992 and 1992–2013). Based on a Kruskal–Wallis test, in the first period, ponds without glaciers presented significantly ($p < 0.01$) higher increases than ponds with glaciers ($+13 \pm 12$ %; 0 ± 3 %, respectively). In contrast, in the second period ponds without glaciers showed higher and significantly ($p < 0.01$) decreases (-38 ± 6 %; -6 ± 2 %, respectively).

Focusing our attention on Fig. 9, this analysis concludes by assessing what we have learned from pond surface areas for the last 50 years. An increase in precipitation occurred until the mid-1990s followed by a decrease until recent years. This is shown, observing the GPCC precipitation series, but it is also confirmed by the behaviour of ponds without glaciers (Fig. 9a). With regard to the glacier melt, until the 1990s, it was constant. Then, an increase occurred in the early 2000s, while in the recent years a decline was observed (Fig. 9b). This is the trend shown by ponds with glaciers. Furthermore, since 1994 the glacier melt, calculated directly from the maximum temperature, which has been recorded by the Pyramid Laboratory, have been fully in agreement with the behaviour of ponds with glaciers. For before 1994, suitable maximum temperature cannot be derived from gridded and reanalysis products (Table 1, Fig. S7), but the ponds demonstrate that the glacier melt in those years has been constant. Simply tracking the glacier surface areas did not yield information on the temporal behaviour of glacier melt. A decrease in glacier surface area has been identified over the last 50 years (Fig. 4c), but this reduction does not correspond to an increase in glacier melt, as normally expected. As discussed by other authors (Thakuri et al., 2014; Salerno et al., 2015; Wagnon et al., 2013), on the south slopes of Mt Everest, the weaker precipitation could be the main cause of glacier shrinkage. In recent years, glaciers are accumulating less than they were decades ago; thus, their size is declining. In contrast, the tracking of pond surface areas demonstrates that glacier melt did not have a trend congruent to

Table 4. Morphometric features of 10 selected ponds considered in the 2000–2013 analysis. Data are from 2013. Coefficients of correlation are for the monsoon season. The relationships with the other seasons are reported in Table S5.

Pond code	Glacier cover (%)	Pond elevation (m a.s.l.)	Basin aspect (°)	Basin slope (°)	Basin area (km^2)	Pond area (10^4 m^2)	Basin elevation (m a.s.l.)	Coefficient of correlation (ponds surface area vs. precipitation)	Coefficient of correlation (ponds surface area vs. glacier melt)
LCN139	1	4749	75	30	0.6	4.6	5596	0.50	0.35
LCN93	2	5244	116	23	0.7	0.6	5502	0.70**	0.39
LCN141	3	5316	152	27	1.4	2.6	5701	0.72**	0.37
LCN11	3	5029	229	24	1.2	1.8	5372	0.76**	0.49
LCN77	7	4920	142	26	8.6	18.3	5507	0.55*	0.29
LCN76	9	4800	140	25	13.6	59.2	5457	0.65**	0.23
LCN24	10	4466	162	28	23.0	54.0	5477	0.44	0.65**
LCN9	13	5202	117	36	0.7	0.6	5792	−0.27	0.61**
LCN3	30	5261	154	35	2.0	11.7	5981	0.17	0.87***
LCN68	32	5006	232	35	1.2	3.2	5686	0.12	0.65**
Median	8	5018	147	28	1.3	3.9	5551	–	–

Significance: *** $p < 0.001$, ** $p < 0.01$, * $p < 0.05$, [a] $p < 0.1$.

the glacier shrinkage, being influence more to the maximum temperature trend.

6 Conclusion

The main contribution provided by this study is to have demonstrated for our case study that surface areas of unconnected ponds could be tracked to detect the behaviour of precipitation and glacier melt in remote and barely accessible regions where, even for recent decades, few or no time series exist. Local end peculiar morphological conditions of each pond (possibly enhanced or reduced sediment supply, landslides, groundwater, etc.) could influence the pond surface area. However, the significant relationships found here on a wide pond population demonstrate that these factors are secondary in respect to the main components of the hydrological cycle.

In high-elevation Himalayan areas, unconnected glacial ponds have demonstrated a high sensitivity to climate change. In general, over the last 50 years (1963–2013), unconnected ponds have decreased significantly by approximately 10 ± 5 %. We attribute this change to both a drop in precipitation and a decrease in glacier melt caused by a decline in the maximum temperature in the recent years. Evaporation has little effect at these elevations and has remained constant over the last decade, during which the main decline in ponds surface area has been observed.

An increase in precipitation occurred until the middle 1990s followed by a decrease until recently. With regard to the glacier melt, until the 1990s it was constant. Then, an increase occurred in the early 2000s, while in recent years a decline has occurred. Simply tracking the glacier surface areas did not yield information on the temporal behaviour of glacier melt. A decrease in glacier surface area has been identified over the last 50 years, attributed by other authors mainly to the observed weaker precipitation. In contrast, the tracking of pond surface areas demonstrates that glacier melt did not have a trend congruent to the glacier shrinkage, being chiefly influenced by the maximum temperature trend.

In conclusion, a question arises in regard to the portability of this method. Here, portability refers to the degree to which the proposed method is replicable in other remote environments. In the Himalaya, other land-based climatic series at high elevations are decidedly scarce (Barry, 2012; Rangwala and Miller, 2012; Pepin et al., 2015; Salerno et al., 2015). The inferences developed here could be simply applied and trends in precipitation and glacier melt were inferred for the overall mountain range. Observing differences in the magnitude of changes between the two classes that differ in glacier coverage (threshold of 10 %) across different periods, along an elevation gradient, or according to the basin aspect, as carried out here, could improve the confidence of the inferred findings. In contrast, in other mountain ranges with other climatic conditions, the inferences developed here might not be valid, and station-observed climatic data would be required to test the ability of glacier ponds to detect the main water balance components.

The Supplement related to this article is available online at doi:10.5194/tc-10-1433-2016-supplement.

Author contributions. Franco Salerno and Gianni Tartari designed research; Franco Salerno, Nicolas Guyennon, and Sudeep Thakuri analysed data; Franco Salerno wrote the paper. Franco Salerno, Nicolas Guyennon, Sudeep Thakuri, Gaetano Viviano, and Gianni Tartari check the data quality.

Acknowledgements. This work was supported by the MIUR through Ev-K2-CNR/SHARE and CNR-DTA/NEXTDATA project within the framework of the Ev-K2-CNR and Nepal Academy of Science and Technology (NAST).

Edited by: G. H. Gudmundsson

References

Adrian, R., O'Reilly, C. M., Zagarese, H., Baines, S. B., Hessen, D. O., Keller, W., Livingstone, D. M., Sommaruga, R., Straile, D., van Donk, E., Weyhenmeyer, G. A., and Winderl, M.: Lakes as sentinels of climate change, Limnol. Oceanogr., 54, 2283–2297, doi:10.4319/lo.2009.54.6_part_2.2283, 2009.

Ageta, Y. and Fujita, K.: Characteristics of mass balance of summer accumulation type glaciers in the Himalayas and Tibetan Plateau, Zeitschrift fur Gletscherkunde und Glazialgeologie, 32, 61–65, 1996

Ageta, Y., Iwata, S., Yabuki, H., Naito, N., Sakai, A., Narama, C., and Karma, T.: Expansion of glacier lakes in recent decades in the Bhutan Himalayas, IAHS Publication, 264, 165–175, 2000.

Amatya, L. K., Cuccillato, E., Haack, B., Shadie, P., Sattar, N., Bajracharya, B., Shrestha, B., Caroli, P., Panzeri, D., Basani, M., Schommer, B., Flury, B., Salerno, F., and Manfredi, E. C.: Improving communication for management of social-ecological systems in high mountain areas: Development of methodologies and tools – The HKKH Partnership Project, Mt. Res. Dev., 30, 69–79, doi:10.1659/MRD-JOURNAL-D-09-00084.1, 2010.

Bajracharya, B., Uddin, K., Chettri, N., Shrestha, B., and Siddiqui, S. A.: Understanding land cover change using a harmonized classification system in the Himalayas: A case study from Sagarmatha National Park, Nepal, Mt. Res. Dev., 30, 143–156, doi:10.1659/MRD-JOURNAL-D-09-00044.1, 2010.

Barry, R. G.: Recent advances in mountain climate research, Theor. Appl. Climatol., 110, 549–553, doi:10.1007/s00704-012-0695-x, 2012.

Benn, D., Wiseman, S., and Hands, K.: Growth and drainage of supraglacial lakes on debris mantled Ngozumpa Glacier, Khumbu Himal, Nepal, J. Glaciol., 47, 626–638, doi:10.3189/172756501781831729, 2001.

Bhuju, D. R., Carrer, M., Gaire, N. P., Soraruf, L., Riondato, R., Salerno, F., and Maharjan, S. R.: Dendroecological study of high altitude forest at Sagarmatha National Park, Nepal, in: Contemporary Research in Sagarmatha (Mt. Everest) Region, Nepal: An Anthology, edited by: Jha, P. K. and Khanal, I. P., Nepal Academy of Science and Technology, Kathmandu, Nepal, 119–130, 2010.

Bolch, T., Buchroithner, M., Pieczonka, T., and Kunert, A.: Planimetric and volumetric glacier changes in the Khumbu Himal, Nepal, since 1962 using Corona, Landsat TM and ASTER data, J. Glaciol., 54, 592–600, doi:10.3189/002214308786570782, 2008.

Bolch, T., Pieczonka, T., and Benn, D. I.: Multi-decadal mass loss of glaciers in the Everest area (Nepal Himalaya) derived from stereo imagery, The Cryosphere, 5, 349–358, doi:10.5194/tc-5-349-2011, 2011.

Bolch, T., Kulkarni, A., Kääb, A., Huggel, C., Paul, F., Cogley, J. G., Frey, H., Kargel, J. S., Fujita, K., Scheel, M., Bajracharya, S., and Stoffel, M.: The state and fate of Himalayan glaciers, Science, 336, 310–314, 2012.

Derin, Y., Anagnostou, E., Berne, A., Borga, M., Boudevillain, B., Buytaert W., Chang, C., Delrieu, G., Hong, Y., Chia Hsu, Y., Lavado-Casimiro, W., Manz, B., Moges, S., Nikolopoulos, E. I., Sahlu, D., Salerno, F., Rodríguez-Sánchez, J., Vergara, H. J., and Yilmaz, K.: Multi-regional Satellite Precipitation Products Evaluation over Complex Terrain, J. Hydrometeorol., doi:10.1175/JHM-D-15-0197.1, online first, 2016.

Fisher, N. I.: Statistical Analysis of Circular Data, Cambridge University Press, Cambridge, UK, 1993.

Fox, J. and Weisberg, S.: An R Companion to Applied Regression, 2nd Edn., Sage, New York, USA, 2011.

Frey, H., Paul, F., and Strozzi, T.: Compilation of a glacier inventory for the western Himalayas from satellite data: methods, challenges and results, Remote Sens. Environ., 124, 832–843, 2012.

Fujita, K., Sakai, A., Nuimura, T., Yamaguchi, S., and Sharma, R.: Recent changes in Imja Glacial lake and its damming moraine in the Nepal Himalaya revealed by in situ surveys and multi-temporal ASTER imagery, Environ. Res. Lett., 4, 1–7, doi:10.1088/1748-9326/4/4/045205, 2009.

Gardelle, J., Arnaud, Y., and Berthier, E.: Contrasted evolution of glacial lakes along the Hindu Kush Himalaya mountain range between 1990 and 2009, Global Planet. Change, 75, 47–55, 2011.

Guyennon, N., Romano, E., Portoghese, I., Salerno, F., Calmanti, S., Petrangeli, A. B., Tartari, G., and Copetti, D.: Benefits from using combined dynamical-statistical downscaling approaches – lessons from a case study in the Mediterranean region, Hydrol. Earth Syst. Sci., 17, 705–720, doi:10.5194/hess-17-705-2013, 2013.

Guzzella, L., Salerno, F., Freppaz, M., Roscioli, C., Pisanello, F., and Poma, G.: POP and PAH contamination in the southern slopes of Mt. Everest (Himalaya, Nepal): Long-range atmospheric transport, glacier shrinkage, or local impact of tourism?, Sci. Total Environ., 544, 382–390, doi:10.1016/j.scitotenv.2015.11.118, 2016.

Hamerlík, L., Svitok, M., Novikmec, M., Očadlík, M., and Bitušík, P.: Local among-site and regional diversity patterns of benthic macroinvertebrates in high altitude waterbodies: do ponds differ from lakes?, Hydrobiologia, 723, 41–52, doi:10.1007/s10750-013-1621-7, 2013.

Hengl, T. and Reuter, H.: How accurate and usable is GDEM?, a statistical assessment of GDEM using LiDAR data, Geomorphometry, 2, 45–48, 2011.

Hervé, M.: Diverse Basic Statistical and Graphical Functions (RVAideMemoire), R package, version 0.9-56, 124 pp., https://cran.r-project.org/web/packages/RVAideMemoire/RVAideMemoire.pdf, last access: 30 June 2016, 2015.

Hock, R.: Temperature index melt modeling in mountain areas, J. Hydrol., 282, 104–115, doi:10.1016/S0022-1694(03)00257-9, 2003.

Hothorn, T., Hornik, K., van de Wiel, M. A., Wiel, H., and Zeileis, A.: Conditional Inference Procedures, R package, version 1.1-2, 98 pp., https://cran.r-project.org/web/packages/coin/coin.pdf, last access: 30 June 2016, 2015.

Ichiyanagi, K., Yamanaka, M. D., Muraji, Y., and Vaidya, B. K.: Precipitation in Nepal between 1987 and 1996, Int. J. Climatol., 27, 1753–1762, doi:10.1002/joc.1492, 2007.

Jensen, M. E. and Haise, H. R.: Estimating evapotranspiration from solar radiation, J. Irrig. Drain. E.-ASCE, 89, 15–41, 1963.

Kääb, A., Berthier, E., Nuth, C., Gardelle, J., and Arnaud, Y.: Contrasting patterns of early twenty-first-century glacier mass change in the Himalayas, Nature, 488, 495–498, doi:10.1038/nclimate1580, 2012.

Kayastha, R. B., Ageta, Y., and Nakawo M.: Positive degree-day factors for ablation on glaciers in the Nepalese Himalayas: Case study on Glacier AX010 in Shorong Himal, Nepal, Bulletins of Glaciological Research, 17, 1–10, 2000.

Kendall, M. G.: Rank Correlation Methods, Oxford University Press, New York, 1975.

Lami, A., Marchetto, A., Musazzi, S., Salerno, F., Tartari, G., Guilizzoni, P., Rogora, M., and Tartari, G. A.: Chemical and biological response of two small lakes in the Khumbu Valley, Himalayas (Nepal) to short-term variability and climatic change as detected by long term monitoring and paleolimnological methods, Hydrobiologia, 648, 189–205, doi:10.1007/s10750-010-0262-3, 2010.

LANDSAT SPPA Team: IDEAS – LANDSAT Products Description Document, Telespazio VEGA UK, available at: https://earth.esa.int/documents/10174/679851/LANDSAT_Products_Description_Document.pdf, last access: 30 June 2016, 2015.

Lei, Y., Yang, K., Wang, B., Sheng, Y., Bird, B. W., Zhang, G., and Tian, L.: Response of inland lake dynamics over the Tibetan Plateau to climate change, Climatic Change, 125, 281–290, doi:10.1007/s10584-014-1175-3, 2014.

Liu, Q., Mayer, C., and Liu S.: Distribution and interannual variability of supraglacial lakes on debris-covered glaciers in the Khan Tengri-Tomur Mountains, Central Asia, Environ. Res. Lett., 10, 4545–4584, doi:10.1088/1748-9326/10/1/014014, 2015.

Loibl, D. M., Lehmkuhl, F., and Grießinger, J.: Reconstructing glacier retreat since the Little Ice Age in SE Tibet by glacier mapping and equilibrium line altitude calculation, Geomorphology, 214, 22–39, doi:10.1016/j.geomorph.2014.03.018, 2014.

Mann, H. B.: Nonparametric tests against trend, Econometrica, 13, 245–259, 1945.

Pathak, P. and Whalen, S.: Using Geospatial Techniques to Analyse Landscape Factors Controlling Ionic Composition of Arctic Lakes, Toolik Lake Region, Alaska, in: Geographic Information Systems: Concepts, Methodologies, Tools, and Applications, edited by Information Resources Management Association, USA, I, 130–150, doi:10.4018/978-1-4666-2038-4.ch012, 2013.

Pepin, N., Bradley, R. S., Diaz, H. F., Baraer, M., Caceres, E. B., Forsythe, N., Fowler, H., Greenword, G., Hashmi, M. Z., Liu, X. D., Miller, J. D., Ning, L., Ohmura, A., Palazzi, E., Rangwala, I., Schoner, W., Severskiy, I., Shahgedoanova, M., Wang, M. B., Williamson, S. N., and Yang D. Q.: Elevation-dependent warming in mountain regions of the world, Nature Climate Change, 5, 424–430, doi:10.1038/nclimate2563, 2015.

Pham, S. V., Leavitt, P. R., McGowan, S., and Peres-Nato, P.: Spatial variability of climate and land-use effects on lakes of the northern Great Plains, Limnol. Oceanogr., 53, 728–742, doi:10.4319/lo.2008.53.2.0728, 2008.

Pohlert, T.: The Pairwise Multiple Comparison of Mean Ranks Package (PMCMR), R package, version 2016-01-06, 27 pp., https://cran.r-project.org/web/packages/PMCMR/vignettes/PMCMR.pdf, last access: 30 June 2016, 2014.

Quincey, D. J., Richardson, S., Luckman, A., Lucas, R., Reynolds, J., Hambrey, M., and Glasser, N.: Early recognition of glacial lake hazards in the Himalaya using remote sensing datasets, Global Planet. Change, 56, 137–152, doi:10.1016/j.gloplacha.2006.07.013, 2007.

Quincey, D. J., Luckman, A., and Benn, D.: Quantification of Everest region glacier velocities between 1992 and 2002, using satellite radar interferometry and feature tracking, J. Glaciol., 55, 596–606, doi:10.3189/002214309789470987, 2009.

R Development Core Team: R: A language and environment for statistical computing, R Foundation for Statistical Computing, Vienna, Austria, available at: http://www.R-project.org, last access: 30 June 2016, 2008.

Rangwala, I. and Miller, J. R.: Climate change in mountains: a review of elevation-dependent warming and its possible causes, Climatic Change, 114, 527–547, doi:10.1007/s10584-012-0419-3, 2012.

Razali, N. M. and Waph, Y. B.: Power comparisons of Shapiro-Wilk, Kolmogorov-Smirnov,Lilliefors and Anderson-Darling tests, Journal of Statistical Modeling and Analytics, 2, 21–33, 2011.

Reynolds, J.: On the formation of supraglacial lakes on debris-covered glaciers, IAHS publication, 264, 153–161, doi:10.3189/002214310791190785, 2000.

Sakai, A.: Glacial lakes in the Himalayas: A review on formation and expansion processes, Global Environmental Research, 16, 23–30, 2012.

Sakai, A. and Fujita, K.: Formation conditions of supraglacial lakes on debris covered glaciers in the Himalaya, J. Glaciol., 56, 177–181, doi:10.3189/002214310791190785, 2010.

Salerno, F., Cuccillato, E., Caroli, P., Bajracharya, B., Manfredi, E. C., Viviano, G., Thakuri, S., Flury, B., Basani, M., Giannino, F., and Panzeri, D.: Experience with a hard and soft participatory modeling framework for social ecological system management in Mount Everest (Nepal) and K2 (Pakistan) protected areas, Mt. Res. Dev., 30, 80–93, doi:10.1659/MRD-JOURNAL-D-10-00014.1, 2010.

Salerno, F., Thakuri, S., D'Agata, C., Smiraglia, C., Manfredi, E. C., Viviano, G., and Tartari, G.: Glacial lake distribution in the Mount Everest region: Uncertainty of measurement and conditions of formation, Global Planet. Change, 92–93, 30–39, doi:10.1016/j.gloplacha.2012.04.001, 2012.

Salerno, F., Viviano, G., Mangredi, E. C., Caroli, P., Thakuri, S., and Tartari, G.: Multiple Carrying Capacities from a management-oriented perspective to operationalize sustainable tourism in protected area, J. Environ. Manage., 128, 116–125, doi:10.1016/j.jenvman.2013.04.043, 2013.

Salerno, F., Gambelli, S., Viviano, G., Thakuri, S., Guyennon, N., D'Agata, C., Diolaiuti, G., Smiraglia, C., Stefani, F., Bochhiola, D., and Tartari, G.: High alpine ponds shift upwards as average temperature increase: A case study of the Ortles-Cevedale mountain group (Southern alps, Italy) over the last 50 years, Global Planet. Change, doi:10.1016/j.gloplacha.2014.06.003, 2014a.

Salerno, F., Viviano, G., Carraro, E., Manfredi, E. C., Lami, A., Musazzi, S., Marchetto, A., Guyennon, N., Tartari, G., and Copetti, D.: Total phosphorus reference condition for subalpine lakes: comparison among traditional methods and a new process based and dynamic lake-basin approach, J. Environ. Manage., 145, 94–105, doi:10.1016/j.jenvman.2014.06.011, 2014b.

Salerno, F., Guyennon, N., Thakuri, S., Viviano, G., Romano, E., Vuillermoz, E., Cristofanelli, P., Stocchi, P., Agrillo, G., Ma, Y., and Tartari, G.: Weak precipitation, warm winters and springs impact glaciers of south slopes of Mt. Everest (central Himalaya) in the last 2 decades (1994–2013), The Cryosphere, 9, 1229–1247, doi:10.5194/tc-9-1229-2015, 2015.

Scherler, D., Bookhagen, B., and Strecker, M. R.: Spatially variable response of Himalayan glaciers to climate change affected by debris cover, Nat. Geosci., 4, 156–159, 2011.

Settle, S., Goonetilleke, A., and Ayoko, G. A.: Determination of Surrogate Indicators for Phosphorus and Solids in Urban Storm water: Application of Multivariate Data Analysis Techniques, Water Air Soil Poll., 182, 149–161, doi:10.1007/s11270-006-9328-2, 2007.

Shapiro, S. S. and Wilk, M. B.: An analysis of variance test for normality (complete samples), Biometrika, 52, 591–611, 1965.

Smith, L. C., Sheng, Y., MacDonald, G. M., and Hinzman, L. D.: Disappearing Arctic Lakes, Science, 308, 1429–1429, doi:10.1126/science.1108142, 2005.

Smol, J. P. and Douglas, M.: From controversy to consensus: Making the case for recent climate change in the Arctic using lake sediments, Front. Ecol. Environ., 5, 466–474, doi:10.1890/060162, 2007a.

Smol, J. P. and Douglas, M. S. V.: Crossing the final ecological threshold in high Arctic ponds, P. Natl. Acad. Sci. USA, 104, 12395–12397, doi:10.1073/pnas.0702777104, 2007b.

Somos-Valenzuela, M. A., McKinney, D. C., Rounce, D. R., and Byers, A. C.: Changes in Imja Tsho in the Mount Everest region of Nepal, The Cryosphere, 8, 1661–1671, doi:10.5194/tc-8-1661-2014, 2014.

Soncini, A., Bocchiola, D., Confortola, G., Minora, U., Vuillermoz, E., Salerno, F., Viviano, G., Shrestha, D., Senese, A., Smiraglia, C., and Diolaiuti, G.: Future hydrological regimes and glacier cover in the Everest region: The case study of the upper Dudh Koshi basin, Sci. Total Environ., doi:10.1016/j.scitotenv.2016.05.138, in press, 2016.

Song, C., Huang, B., Richards, K., Ke, L., and Phan, V. H.: Accelerated lake expansion on the Tibetan Plateau in the 2000s: Induced by glacial melting or other processes?, Water Resour. Res., 50, 3170–3186, doi:10.1002/2013WR014724, 2014.

Song, C., Huang, B., and Ke, L.: Heterogeneous change patterns of water level for inland lakes in High Mountain Asia derived from multi-mission satellite altimetry, Hydrol. Process., 29, 2769–2781, doi:10.1002/hyp.10399, 2015.

Tachikawa, T., Kaku, M., Iwasaki, A., Gesch, D., Oimoen, M., Zhang, Z., Danielson, J., Krieger, T., Curtis, B., Haase, J., Abrams, M., Crippen, R., and Carabajal, C.: ASTER Global Digital Elevation Model Version 2 – Summary of Validation Results, NASA Land Processes Distributed Active Archive Center and the Joint Japan-US ASTER Science Team, available at: https://lpdaacaster.cr.usgs.gov/GDEM/Summary_GDEM2_validation_report_final.pdf, last access: 30 June 2016, 2011.

Tartari, G. Previtali, L., and Tartari, G. A.: Genesis of the lake cadastre of Khumbu Himal Region (Sagarmatha National Park, East Nepal), in: Limnology of high altitude lakes in the Mt Everest Region (Nepal), edited by: Lami, A., and Giussani, G., Memorie dell'Istituto italiano di idrobiologia dott. Marco De Marchi, 57, 139–149, 1998.

Tartari, G., Salerno, F., Buraschi, E., Bruccoleri, G., and Smiraglia, C.: Lake surface area variations in the North-Eastern sector of Sagarmatha National Park (Nepal) at the end of the 20th Century by comparison of historical maps, J. Limnol., 67, 139–154, doi:10.4081/jlimnol.2008.139, 2008.

Thakuri, S., Salerno, F., Smiraglia, C., Bolch, T., D'Agata, C., Viviano, G., and Tartari, G.: Tracing glacier changes since the 1960s on the south slope of Mt. Everest (central Southern Himalaya) using optical satellite imagery, The Cryosphere, 8, 1297–1315, doi:10.5194/tc-8-1297-2014, 2014.

Thakuri, S., Salerno, F., Bolch, T., Guyennon, N., and Tartari, G.: Factors controlling the accelerated expansion of Imja Lake, Mount Everest region, Nepal, Ann. Glaciol., 57, 245–257, doi:10.3189/2016AoG71A063, 2016.

Venables, W. N. and Ripley, B. D.: Modern Applied Statistics with S, Springer, New York, 2002.

Viviano, G., Salerno, F., Manfredi, E. C., Polesello, S., Valsecchi, S., and Tartari, G.: Surrogate measures for providing high frequency estimates of total phosphorus concentrations in urban watersheds, Water Res., 64, 265–277, doi:10.1016/j.watres.2014.07.009, 2014.

Vuille, M.: Climate variability and high altitude temperature and precipitation, in: Encyclopedia of snow, ice and glaciers, edited by: Singh, V. P., Singh, P., and Haritashya, U. K., Springer, 153–156, 2011.

Wagnon, P., Vincent, C., Arnaud, Y., Berthier, E., Vuillermoz, E., Gruber, S., Ménégoz, M., Gilbert, A., Dumont, M., Shea, J. M., Stumm, D., and Pokhrel, B. K.: Seasonal and annual mass balances of Mera and Pokalde glaciers (Nepal Himalaya) since 2007, The Cryosphere, 7, 1769–1786, doi:10.5194/tc-7-1769-2013, 2013.

Wang, W., Xiang, Y., Gao, Y., Lu, A., and Yao, T.: Rapid expansion of glacial lakes caused by climate and glacier retreat in the Central Himalayas, Hydrol. Process., 29, 859–874, doi:10.1002/hyp.10199, 2015.

Williamson, C. E., Dodds, W., Kratz, T. K., and Palmer, M.: Lakes and streams as sentinels of environmental change in terrestrial and atmospheric processes, Front. Ecol. Environ., 6, 247–254, doi:10.1890/070140, 2008.

Willmott, C. and Matsuura, K.: Advantages of the Mean Absolute Error (MAE) over the Root Mean Square Error (RMSE) in assessing average model performance, Clim. Res., 30, 79–82, doi:10.3354/cr030079, 2005.

Wold, S., Esbensen, K., and Geladi, P.: Principal component analysis, Chemometrics and Intelligent Laboratory Systems, 2, 37–52, 1987.

Xie, A., Ren, J., Qin, X., and Kang, S.: Reliability of NCEP/NCAR reanalysis data in the Himalayas/Tibetan Plateau, J. Geogr. Sci., 17, 421–430, doi:10.1007/s11442-007-0421-2, 2007.

Yao, T., Thompson, L., Yang, W., Yu, W., Gao, Y., Guo, X., Yang, X., Duan, K., Zhao, H., Xu, B., Pu, J., Lu, A., Xiang, Y., Kattel, D. B., and Joswiak, D.: Different glacier status with atmospheric circulations in Tibetan Plateau and surroundings, Nature Climate Change, 2, 663–667, doi:10.1038/nclimate1580, 2012.

Zhang, G., Yao, T., Xie, H., Wang, W., and Yang, W.: An inventory of glacial lakes in the Third Pole region and their changes in response to global warming, Global Planet. Change, 131, 148–157, doi:10.1016/j.gloplacha.2015.05.013, 2015.